Journal of Fluorine Chemistry 135 (2012) 59–67

Contents lists available at SciVerse ScienceDirect

Journal of Fluorine Chemistry

journal homepage: www.elsevier.com/locate/fluor

An in-depth *in situ* IR study of the thermal decomposition of copper trifluoroacetate hydrate

M. Mosiadz [a,*], K.L. Juda [a,b], S.C. Hopkins [a], J. Soloducho [b], B.A. Glowacki [a,c]

[a] Department of Materials Science and Metallurgy, University of Cambridge, Pembroke Street, Cambridge, CB2 3QZ, United Kingdom
[b] Department of Chemistry, Wroclaw University of Technology, Wybrzeze Wyspianskiego 27, 50-370 Wroclaw, Poland
[c] Institute of Power Engineering, ul. Augustowka 6, 02-981 Warsaw, Poland

ARTICLE INFO

Article history:
Received 8 April 2011
Received in revised form 12 August 2011
Accepted 16 August 2011
Available online 30 August 2011

Keywords:
Copper trifluoroacetate
Copper oxide
Hexafluoropropylene oxide (HFPO)
HR-TG
FT-IR
DSC

ABSTRACT

The pyrolysis of $Cu(CF_3COO)_2{\cdot}nH_2O$ at temperatures up to 1000 °C, under flowing pure Ar, O_2 and O_2 saturated with water vapour, was extensively analysed. Decomposition reaction paths in all three media are proposed and various solid intermediates and gaseous products are identified. $Cu_2(CF_3COO)_3(OH)$ and $Cu(CF_3COO)_2{\cdot}CuO$ formed sequentially, liberating TFAH at both stages. $Cu(CF_3COO)_2{\cdot}CuO$ decomposition occurred in a single endothermic step with an onset temperature of 263 °C in flowing dry Ar, but proceeded by a violent, exothermic and multistage route with onset temperatures of 216 and 209 °C in flowing dry O_2 and wet O_2 respectively, in all cases forming CuO. The formation of HF was also observed directly and the existence of a:CF_2 radical inferred. The onset temperatures of the main decomposition are significantly lower than previously reported. This observation, and the violent exothermic nature of the decomposition in O_2 atmospheres, are suggested to have implications for sol–gel processing.

1. Introduction

Trifluoroacetate salts are the most popular precursors for yttrium, barium and copper in the synthesis of superconducting $YBa_2Cu_3O_{7-\delta}$ Coated Conductors (YBCO CC), as they inhibit the formation of carbon-rich impurities, for example $BaCO_3$, during post-deposition heat treatment [1,2]. They have been successfully used in YBCO CC thin film deposition [3,4] via a sol–gel method (Chemical Solution Deposition, CSD). Unlike Physical Vapour Deposition (PVD) techniques, which often require ultra-high vacuum, the sol–gel approach is cheap and can be easily scaled up. Although controlling the chemical composition of a film is straightforward in comparison to PVD methods, optimising the crucial transformation of the deposited gel into a film with the right morphology is challenging. In particular, porosity and the segregation of Cu species have often been reported to arise during pyrolysis of TFA-derived YBCO precursors, and this has been attributed to high heating rates and rapid HF release [5]. This has motivated the development of fluorine-free routes [6], but it has also been reported that porosity can be avoided with TFA-derived precursors through careful control of the atmosphere and temperature profile during pyrolysis [7]. A thorough analysis and understanding of the decomposition process can contribute to controlling this transformation and optimising the material's final performance.

Although widely used, surprisingly little has been reported about the copper trifluroacetate salt's structure and almost nothing regarding its thermal decomposition. Neither anhydrous nor hydrated copper trifluoroacetate assume a binuclear configuration like copper acetate, but UV visible reflectance and IR spectra together with magnetic susceptibility strongly suggest that the salt may have a polymeric structure [8–11]. Although there is no interaction between metal cations, a strong cation–anion interaction between copper and organic solvent molecules, e.g. diethyl ether, benzene, nitromethane, strong acid anions and chloride, has been reported [9,12].

In the present work we present the results of an in-depth *in situ* IR study of the thermal decomposition of copper trifluoroacetate hydrate, as a full understanding of pyrolysis is of great importance during any sol–gel deposition technique.

2. Experimental

2.1. Chemicals

Copper(II) trifluoroacetate hydrate (Cu-TFA, $Cu(CF_3COO)_2{\cdot}nH_2O$) was obtained from Alfa Aesar (JM) and used as supplied. The manufacturer's certificate of analysis for this lot specified $n = 0.56$,

* Corresponding author. Tel.: +44 1223 767933; fax: +44 1223 334567.
E-mail address: mm701@cam.ac.uk (M. Mosiadz).

0022-1139/$ – see front matter © 2011 Elsevier B.V. All rights reserved.
doi:10.1016/j.jfluchem.2011.08.010

determined by EDTA titration in the presence of SNAZOXS as an indicator.

2.2. Characterisation techniques

Thermogravimetry (TG) and High Resolution Thermogravimetry (HR-TG) coupled with Fourier Transform Infrared (FT-IR) Spectroscopy were performed using a TA Instruments TGA Q500 in an open platinum crucible. For standard TG, a heating rate of 5 °C/min was used from room temperature to 1000 °C. HR-TG was performed up to 600 °C, with a heating rate dynamically adjusted in response to the measured rate of change of mass in the range from 0 to 20 °C/min. Analysed samples were between 5 and 10 mg in mass each. The mixture of evolved and purge gases was transferred to the heated stainless steel gas cell of a Thermo Scientific Nicolet iS10 Spectrometer via glass-lined stainless steel tubing, which was also heated to around 125 °C to avoid the condensation of less volatile species. Spectra were recorded at appropriate intervals throughout each run with 4 cm^{-1} resolution. All data collected from TG and HR-TG were analysed in TA Universal Analysis software, and differentiated to obtain Differential Thermogravimetry (DTG) data; and all data collected from FT-IR were analysed in Thermo Scientific Omnic software. The start of a reaction was defined from the mass vs temperature curve by the intersection of the extrapolated local horizontal baseline and the tangent to the curve at its steepest point [13]. The equipment was purged before each measurement for 0.5 h at ambient temperature before a background IR spectrum was taken.

Simultaneous Thermogravimetry and Differential Scanning Calorimetry (TG-DSC) were performed using a TA Instruments SDT Q600 in an open platinum crucible with a heating rate of 5 °C/min from room temperature to 1000 °C. Analysed samples were between 5 and 10 mg in mass each. Data were analysed in TA Universal Analysis software, with the same definition of the start of a reaction as used for TG. Results are presented here using the convention of a positive peak in the temperature difference between the sample and the reference for an exothermic process and a negative trough for an endothermic process.

The TG, HR-TG and TG-DSC measurements were performed in three different atmospheres with a flow rate of 100 mL/min: pure Ar, O_2, and O_2 saturated with water vapour. The high-purity compressed Ar and O_2 gases were first dried using silica gel. The water-saturated O_2 atmosphere was prepared at standard temperature and pressure (25 °C, 1 atm). Every experiment was repeated 3 times in order to confirm the results and gain enough powder for X-ray Diffractometry and Scanning Electron Microscopy.

X-ray Diffractometry (XRD) was performed on powder samples using Philips X'Pert PW1730 diffractometers. The instruments used the Bragg-Brentano geometry and unfiltered Cu K_α radiation. $\theta/2\theta$ scans were performed with 1/2° divergence and anti-scatter slits and a 0.3 mm receiving slit to minimise variations in measured intensity as a result of the finite sample area (typically 1 cm^2). All powder diffraction data were analysed in Panalytical Highscore Plus software and compared with the International Centre for Diffraction Data (ICDD) powder diffraction file PDF2. Semi-quantitative phase analysis was performed by Rietveld refinement.

Scanning Electron Microscopy (SEM) was performed on powder samples using a JEOL JSM 5800 LV Scanning Microscope with a W source and an ultra-thin window (UTW) detector for Energy Dispersive X-ray (EDX) spectroscopy. The detector was calibrated each time against Si. All SEM images and EDX data were analysed in INCA software.

Fourier Transform Infrared (FT-IR) Spectroscopy for powder samples was performed using a Bruker Tensor 27 FT-IR Spectrometer in transmission mode. Samples were prepared as pellets containing anhydrous KBr. The results were analysed in OPUS software.

3. Results

The results of thermogravimetric analysis revealed a number of distinct regions of mass loss. The first, starting around 70 °C, was associated with a single peak in DTG. The second mass loss starting around 135 °C corresponded to a couple of poorly resolved peaks for both dry Ar and pure O_2 atmospheres. The third, and the largest, mass loss started at 268 and 212 °C for dry Ar and pure O_2 atmospheres respectively, and was represented by a very sharp and dominant peak in the DTG in the case of a flowing dry Ar atmosphere. For the pure O_2 atmosphere, however, a very broad peak in DTG was present. An additional mass loss from 770 °C to 825 °C was present for the dry Ar atmosphere only, and is associated with a broad peak in DTG (Fig. 1). After TG, a solid deposit was observed outside the crucible in both atmospheres used here, suggesting that the vaporisation of a copper species occurred inside the heating cell.

In order to resolve these overlapping peaks and to identify the evolved gases of decomposition, the compound was subjected to HR-TG coupled with FT-IR in three different purge gases: dry Ar, pure O_2 and O_2 saturated with water vapour. Fig. 2 shows the full temperature range of HR-TG data in dry Ar and O_2 atmospheres; the results in the wet and dry O_2 atmospheres were almost identical. The first features are two sharp mass losses at 77, 83 and 87 °C, and at 143, 149 and 149 °C, for dry Ar, dry O_2 and wet O_2 respectively, corresponding to two spikes in DTG. The mass continued to decrease slowly with a changing rate up to the main decomposition step at a temperature of 263, 216 and 209 °C for dry Ar, dry O_2 and wet O_2 respectively, and was associated with the very broad and unresolved features in DTG.

It was confirmed by repeated FT-IR analysis, as described later, that the stepwise mass loss up to the main decomposition step

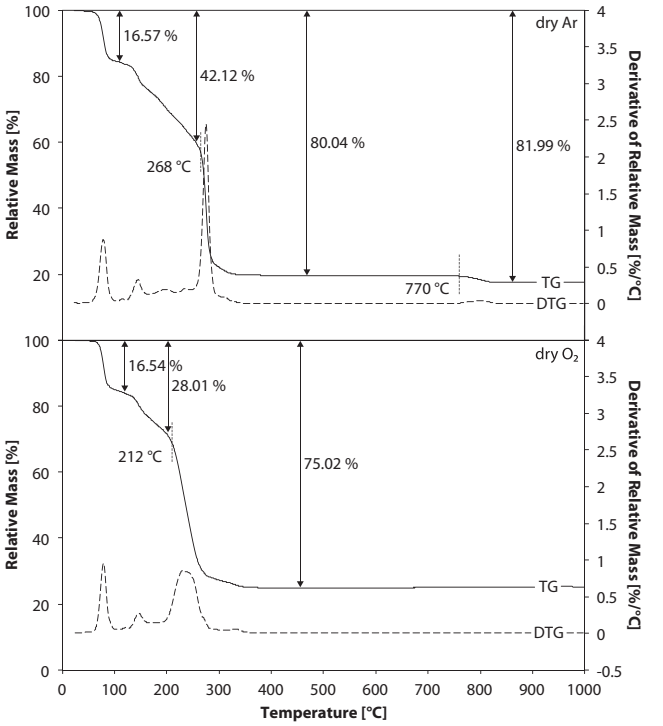

Fig. 1. TG and DTG curves of Cu-TFA heated at 5 °C/min under a flowing dry Ar (top) and dry O_2 (bottom) atmosphere, revealing several partially overlapping processes resulting in mass loss.

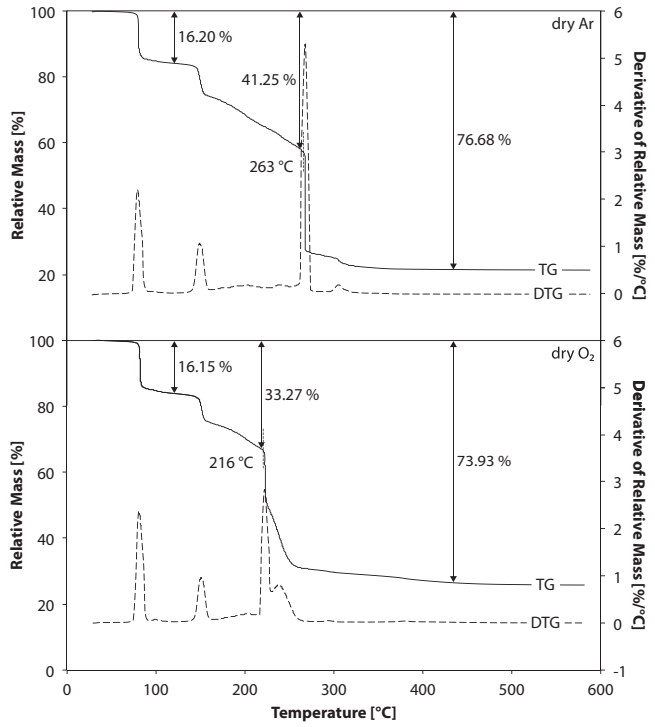

Fig. 2. HR-TG and DTG curves of Cu-TFA heated under a flowing dry Ar (top) and dry O_2 (bottom) atmosphere, with the sequence of mass loss stages more clearly resolved. After the last major decomposition step, corresponding to $Cu(CF_3COO)_2{\cdot}CuO$ decomposition, identical curves were recorded under flowing dry and wet O_2 atmospheres.

Table 1
Semi-quantitative XRD data for the solid products of heating Cu-TFA to 1000 °C at 5 °C/min during TG. The values are estimated based on Rietveld refinement.

Compound	Composition (wt %)	
	Dry Ar	Dry O_2
CuO	15.9	100
Cu_2O	84.1	–

corresponded almost exclusively to pure TFAH liberation, and not the expected loss of the water of crystallisation. The first mass loss also occurs close to the boiling point of TFAH, 72.4 °C. Based on these observations and the first two mass losses, two intermediate species can be proposed: a monohydroxy binuclear complex of Cu^{2+} and a CF_3COO^- group in the form of $Cu_2(CF_3COO)_3(OH)$, and a complex compound of Cu^{2+}, a CF_3COO^- group and copper(II) oxide (CuO) in the form of $Cu(CF_3COO)_2{\cdot}CuO$, respectively (Tables 2 and 3).

The rapid decomposition of what is believed to be $Cu(CF_3COO)_2{\cdot}CuO$ began at 263 °C, for the dry Ar atmosphere only, and resulted in a sharp mass loss, reaching a horizontal plateau at 360 °C. In this temperature range, the corresponding DTG curve has only one very intense peak, revealing a rapid single-step decomposition mechanism. For the dry and wet O_2 atmospheres, the rapid decomposition of $Cu(CF_3COO)_2{\cdot}CuO$ began at a temperature about 50 °C lower than for the dry Ar atmosphere; an initially sharp mass loss was followed by more gradual mass loss, reaching a horizontal plateau at 440 and 370 °C, respectively. In this region, the corresponding DTG curves have two overlapping peaks, revealing a rapid two-stage decomposition mechanism (Fig. 2). In all flowing atmospheres, TG revealed a small additional weight loss just before the curve reached a horizontal plateau after the main decomposition step: in all cases, the remaining mass after decomposition is taken

Table 2
TG data for Cu-TFA decomposition at a 5 °C/min heating rate, showing the relative remaining mass after hydrolysis of the salt, the sequential decomposition of $Cu_2(CF_3COO)_3(OH)$ and $Cu(CF_3COO)_2{\cdot}CuO$, and CuO reduction. The theoretical values are calculated on the assumption that the starting material is a partially hydrated salt ($n = 0.5$) and that the sole solid products are $Cu(CF_3COO)_2{\cdot}CuO$, CuO and Cu_2O for the decomposition of $Cu_2(CF_3COO)_3(OH)$, $Cu(CF_3COO)_2{\cdot}CuO$ and CuO respectively.

Compound	Flowing atmosphere	Hydrolysis temperature (°C)	Mass % as $Cu_2(CF_3COO)_3$ (OH)		Decomposition temperature (°C)	Mass % as $Cu(CF_3COO)_2{\cdot}CuO$		Decomposition temperature (°C)	Mass % as CuO		Reduction temperature (°C)	Mass % as Cu_2O	
			Theory	Found		Theory	Found		Theory	Found		Theory	Found
$2Cu(CF_3COO)_2\ 0.5H_2O$	Dry Ar	69	80.91	83.47	133	61.81	57.88	268	26.64	19.96	770	23.96	18.01
	Dry O_2	71	80.91	83.46	137	61.81	71.99	212	26.64	24.98	–	–	–

Table 3
HR-TG data for Cu-TFA decomposition, showing the relative remaining mass after hydrolysis of the salt, and the sequential decomposition of $Cu_2(CF_3COO)_3(OH)$ and $Cu(CF_3COO)_2{\cdot}CuO$. The theoretical values are calculated on the assumption that the starting material is a partially hydrated salt ($n = 0.5$) and that the sole solid products are $Cu(CF_3COO)_2{\cdot}CuO$ and CuO for the decomposition of $Cu_2(CF_3COO)_3(OH)$ and $Cu(CF_3COO)_2{\cdot}CuO$.

Compound	Flowing atmosphere	Hydrolysis temperature (°C)	Mass % as $Cu_2(CF_3COO)_3$ (OH)		Decomposition temperature (°C)	Mass % as $Cu(CF_3COO)_2{\cdot}CuO$		Decomposition temperature (°C)	Mass % as CuO	
			Theory	Found		Theory	Found		Theory	Found
$2Cu(CF_3COO)_2{\cdot}0.5H_2O$	Dry Ar	77	80.91	83.80	143	61.81	58.75	263	26.64	23.32
	Dry O_2	83	80.91	83.85	149	61.81	66.73	216	26.64	26.07
	Wet O_2	87	80.91	83.41	149	61.81	61.60	209	26.64	26.05

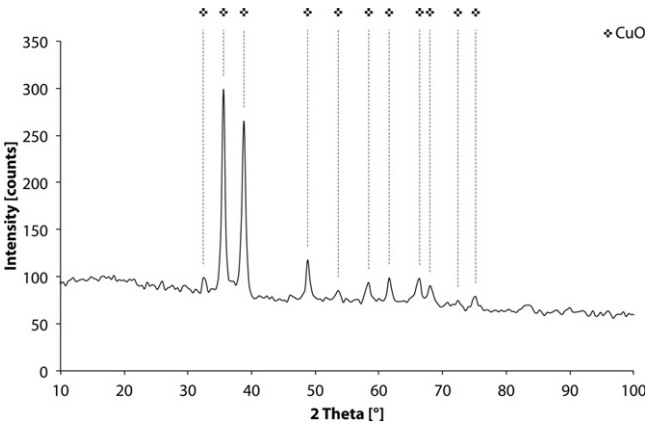

Fig. 3. XRD 2θ scan (Cu K_α) of the residue after heating Cu-TFA to 600 °C under a flowing dry Ar atmosphere during HR-TG, revealing copper(II) oxide (CuO) formation; identical patterns were recorded for the powder samples obtained under flowing dry and wet O_2 atmospheres.

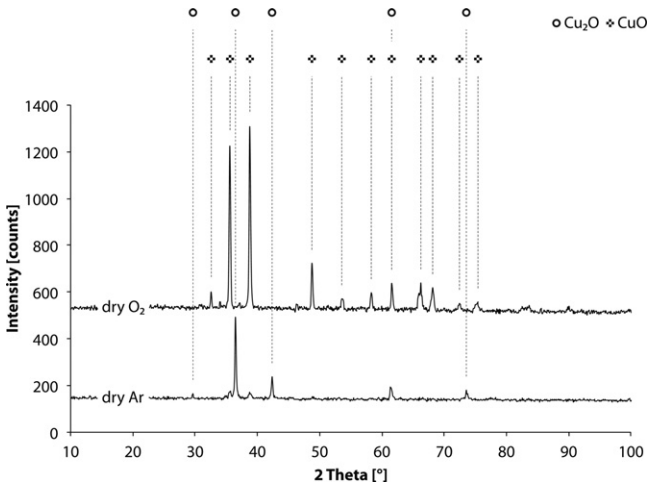

Fig. 4. XRD 2θ scans (Cu K_α) of the residues after heating Cu-TFA to 1000 °C at 5 °C/min under flowing dry atmospheres during TG, revealing the formation of pure copper(II) oxide (CuO) in dry O_2, and a mixture of CuO and copper(I) oxide (Cu_2O) in dry Ar. The results in wet and dry O_2 atmospheres were identical.

after this point. The start temperatures of the main decomposition, and the remaining masses for all investigated conditions, are listed in Table 3. After this decomposition no further mass changes were observed up to the maximum temperature of 600 °C reached in HR-TG. The remaining mass after $Cu(CF_3COO)_2{\cdot}CuO$ decomposition is in good agreement with that expected for CuO for the O_2 atmospheres, but in flowing dry Ar a lower remaining mass was observed. This is consistent with the observation that one or more copper species vaporised. The additional mass loss observed in TG only in a flowing dry Ar atmosphere, over a 55 °C range starting at 770 °C, suggests the reduction of CuO to Cu_2O (Table 2).

In order to confirm the products remaining after decomposition, samples were collected for XRD. Fig. 3 shows the diffraction pattern of the black powder remaining after HR-TG was performed up to a temperature of 600 °C, demonstrating that this product was CuO. EDX analysis of the same powder confirmed the O/Cu atomic ratio to be 0.89 ± 0.02 and 0.95 ± 0.02 for dry Ar and both O_2 atmospheres, respectively (Fig. 5). Transmission FT-IR was also performed on the powder residues after HR-TG to test for the presence of organic species: none were found. The remaining powders collected after TG was performed up to a temperature of 1000 °C in flowing dry Ar and pure O_2 atmospheres were clearly different, being violet-red in the former atmosphere and black in the latter. The red powder was identified by XRD as a mixture of CuO and copper(I) oxide (Cu_2O); the black powder was pure CuO, as before (Fig. 4). This confirms that reduction of CuO occurred in the flowing

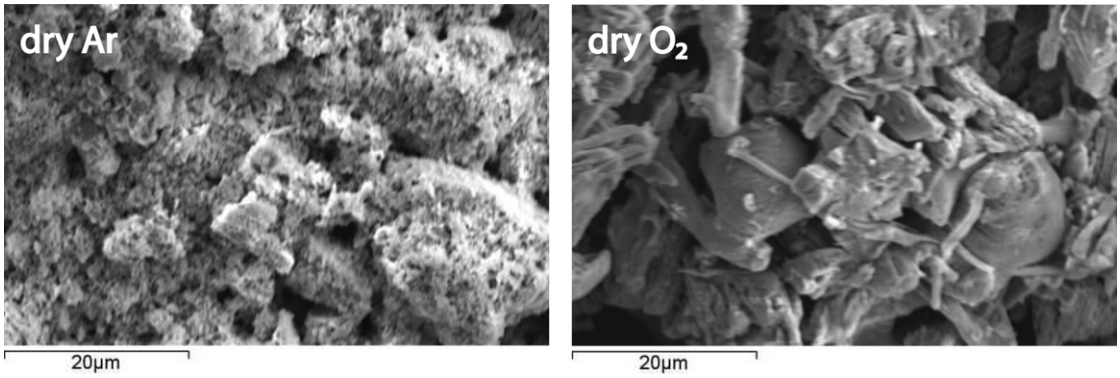

Fig. 5. SEM micrographs (secondary electron images) of the products of Cu-TFA decomposition after HR-TG under flowing dry Ar (left) and O_2 (right) atmospheres, revealing significant difference in the surface morphology (porosity) of the particles. EDX analysis suggested O/Cu atomic ratios of 0.89 ± 0.02 and 0.96 ± 0.02 for the dry Ar and O_2 atmospheres respectively.

Table 4
Assignment of IR peaks (4000–400 cm^{-1}) recorded during HR-TG of Cu-TFA under a flowing dry Ar atmosphere.

Observed peak (cm^{-1})	Species	Approximate description	Reference
3920	HF	H–F	[14,15]
3877	HF	H–F	[14,15]
3833	HF	H–F	[14,15]
3788	HF	H–F	[14,15]
3726	CO_2	C=O	[16]
3700	CO_2	C=O	[16]
3627	CO_2	C=O	[16]
3579	CF_3COOH	O–H str	[14,16–18]
2362	CO_2	C=O asym str	[14,16]
2337	CO_2	C=O asym str	[14,16]
2178	CO	C≡O	[14,16]
2111	CO	C≡O	[14,16]
1829	CF_3COOH	C=O str	[14,16–18]
1405	CF_3COOH	C–O str	[14,16–18]
1375	CHF_3	C–F str	[14,16]
1234	CF_3COOH	C–F asym str	[14,16–18]
1203	CF_3COOH	C–F sym str C–C str	[14,16–18]
1151	CHF_3	C–F str	[14,16]
1120	CF_3COOH	O–H ip def	[14,16–18]
1026	SiF_4	Si–F str	[19–21]
778	CF_3COOH	C–C ip def	[14,16–18]
667	CO_2 CF_3COOH	C=O def	[16–18]
580	CF_3COOH	C–F ip sym def	[14,16–18]

str = stretching, def = deformation.
sym = symmetric, asym = asymmetric.
ip = in-plane, oop = out-of-plane.

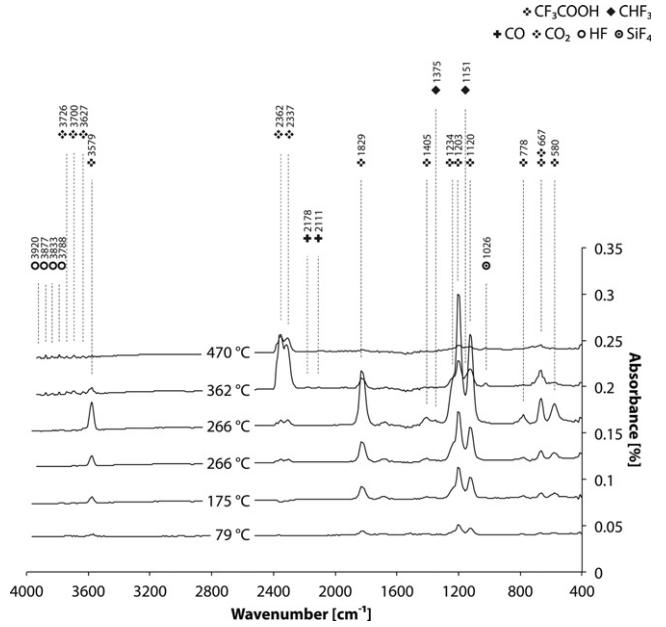

Fig. 6. FT-IR spectra of gases evolved during HR-TG of Cu-TFA under a flowing dry Ar atmosphere, revealing liberation of CF_3COOH, HF, CO_2, CHF_3, CO and SiF_4 at the indicated temperatures (curves offset for clarity).

dry Ar atmosphere at a temperature above 600 °C. The approximate composition determined by Rietveld refinement is shown in Table 1; but as the ratio of remaining masses before and after the final mass loss is consistent with complete reduction, it is likely that the small amount of CuO formed by subsequent oxidation during cooling.

A mixture of carbon dioxide (CO_2), carbon monoxide (CO) and fluorinated compounds were identified by FT-IR analysis during heating in a flowing dry Ar atmosphere (Fig. 6). The evolution of CO_2 and CO is represented by the carbonyl stretch at 3726, 3700, 3627, 2362, 2337, 667 cm^{-1} and peaks at 2178 and 2111 cm^{-1}, respectively. The fluorinated mixture consisted of trifluoroacetic acid (TFAH) and trifluoromethane (CHF_3). The principal changes in spectrum with temperature are the changes in intensity of the TFAH peaks at 3579, 1829, 1405, 1234, 1203, 1120, 778, 667 and 580 cm^{-1} as well as CHF_3 peaks at 1375 and 1151 cm^{-1}, associated with carbonyl (C=O), C–H, C–C and C–F stretches listed in Table 4. The peaks at 3920, 3877, 3833 and 3788 cm^{-1} are evidence of the presence of hydrogen fluoride (HF) in the gas mixture. A peak at 1026 cm^{-1} develops for silicon tetrafluoride (SiF_4), which is believed to be a reaction product between HF and either the quartz elements of the furnace tube or the glass spectroscopic cell [14,26]. Repeated analysis did not identify any trifluoroacetic anhydride (TFAA) or its decomposition products, trifluoroacetyl fluoride (CF_3COF) and carbonyl fluoride (COF_2), in the evolved gas mixture [27]. A list of all species recognised in a flowing dry Ar atmosphere is presented in Table 4 together with the assigned stretching regions and references.

In addition to all species identified in a flowing dry Ar atmosphere, characteristic peaks of hexafluoropropylene oxide ($CF_3(CFCF_2)O$, HFPO) and carbonyl fluoride (COF_2) were recognised by FT-IR in both flowing O_2 atmospheres (Fig. 7). The formation of HFPO is observed from the peaks at 1282, 1234 and 1161 cm^{-1}, and the peaks at 1957, 1928, 1269 and 617 cm^{-1} are evidence of the presence of COF_2 in the gas mixture. Repeated analysis confirmed the absence of TFAA and CF_3COF from the evolved gas mixture. A list of all species recognised in both O_2 atmospheres is presented in Table 5 together with the assigned stretching regions and references.

The rate of evolution of each detected species, as reflected by the absorbance in the FT-IR data, depended on the temperature and atmosphere (Figs. 6 and 7). For all the atmospheres used, TFAH evolution began near its boiling point and proceeded stepwise to the main $Cu(CF_3COO)_2{\cdot}CuO$ decomposition. In a dry Ar atmosphere, the evolution of TFAH (and no other species) peaked sharply at the onset temperature for $Cu(CF_3COO)_2{\cdot}CuO$ decomposition identified by HR-TG (263 °C); CO_2 release began slowly shortly afterwards and increased continuously in intensity, peaking around 360 °C (Fig. 8). This suggests that TFAH is the

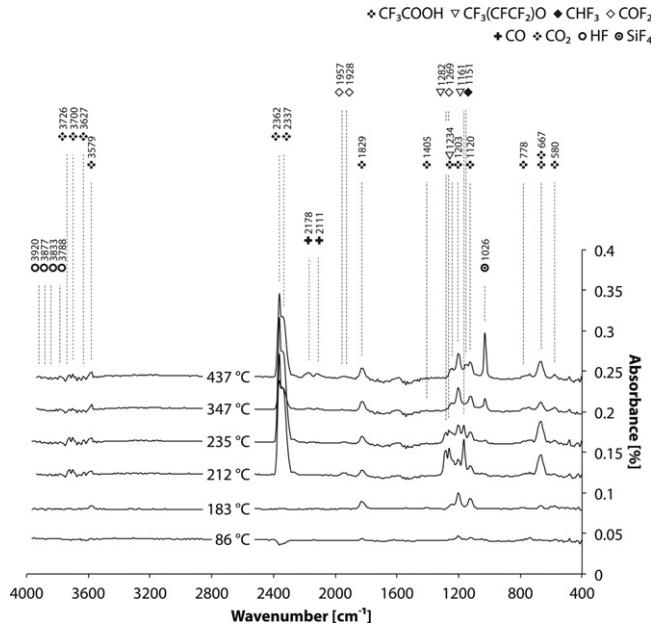

Fig. 7. FT-IR spectra of gases evolved during HR-TG of Cu-TFA under a flowing wet O_2 atmosphere, revealing liberation of $CF_3(CFCF_2)O$, COF_2, CO_2, CF_3COOH, HF, CHF_3, SiF_4 and CO at the indicated temperatures (curves offset for clarity).

Table 5
Assignment of IR peaks (4000–400 cm^{-1}) recorded during HR-TG of Cu-TFA under a flowing wet O_2 atmosphere.

Observed peak (cm^{-1})	Species	Approximate description	Reference
3920	HF	H–F	[14,15]
3877	HF	H–F	[14,15]
3833	HF	H–F	[14,15]
3788	HF	H–F	[14,15]
3726	CO_2	C=O	[16]
3700	CO_2	C=O	[16]
3627	CO_2	C=O	[16]
3579	CF_3COOH	O–H str	[14,16–18]
2362	CO_2	C=O asym str	[14,16]
2337	CO_2	C=O asym str	[14,16]
2178	CO	C≡O	[14,16]
2111	CO	C≡O	[14,16]
1957	COF_2	C=O str	[22,23]
1928	COF_2	C=O str	[22,23]
1829	CF_3COOH	C=O str	[14,16–18]
1405	CF_3COOH	C–O str	[14,16–18]
1282	$CF_3(CFCF_2)O$	C–F str	[14,24,25]
1269	COF_2	C–F str	[22,23]
1234	CF_3COOH $CF_3(CFCF_2)O$	C–F asym str	[14,16–18] [14,24,25]
1203	CF_3COOH	C–C str C–F sym str	[14,16–18]
1161	$CF_3(CFCF_2)O$	C–F str	[14,24,25]
1151	CHF_3	C–F str	[14,16]
1120	CF_3COOH	O–H ip def	[14,16–18]
1026	SiF_4	Si–F str	[19–21]
778	CF_3COOH	C–C ip def	[14,16–18]
667	CO_2 CF_3COOH	C=O def	[16–18]
649	CF_3COOH	C=O def	[16,18]
580	CF_3COOH	C–F ip sym def	[14,16–18]

str = stretching, def = deformation.
sym = symmetric, asym = asymmetric.
ip = in-plane, oop = out-of-plane.

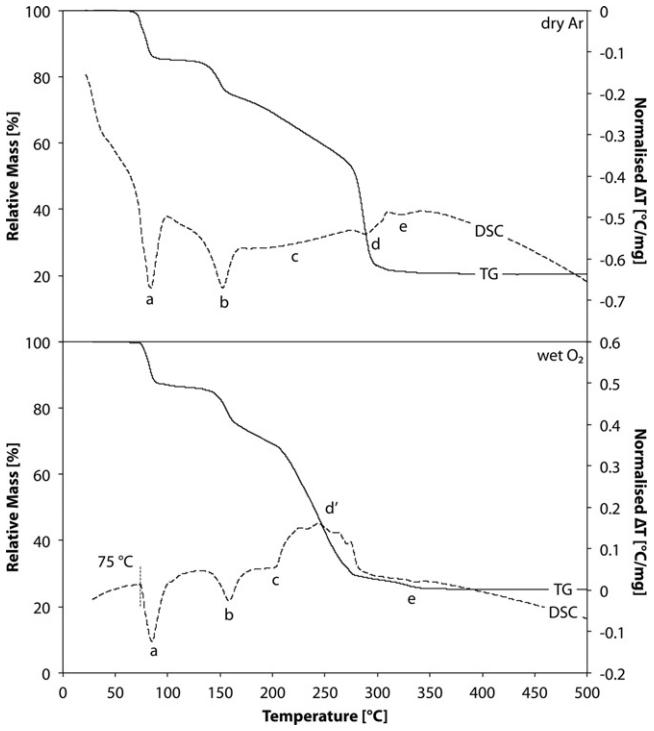

Fig. 9. TG and DSC (exothermic positive) curves of Cu-TFA heated at 5 °C/min under flowing dry Ar (top) and wet O_2 (bottom) atmospheres, revealing three stages of endothermic TFAH evaporation (a, b and c), followed by the endothermic single stage (d) and exothermic multistage (d′) decomposition of $Cu(CF_3COO)_2{\cdot}CuO$, and a small endothermic peak (e) for the final loss of organic species in the formation of CuO. Identical curves were recorded under flowing dry and wet O_2 atmospheres.

only volatile product of the decomposition in an inert atmosphere. The delayed detection of CO_2, which coincides with CHF_3 and HF, might suggest that these species arise from decomposition of the acid (Fig. 6, Fig. 8). Traces of SiF_4 were also identified.

In contrast, in the flowing O_2 atmospheres the TFAH concentration barely increased at the onset of $Cu(CF_3COO)_2{\cdot}CuO$ decomposition (around 210 °C). Instead, a sharp peak in the amount of three species – HFPO, COF_2 and CO_2 – was detected, indicating a clear difference in the decomposition reaction path (Figs. 7 and 8). Above 360 °C, a significant amount of CHF_3 was detected, coinciding with a broad peak in CO_2 evolution; and a growing amount of SiF_4 was detected, becoming the most intense signal after CO_2 at the highest measured temperatures.

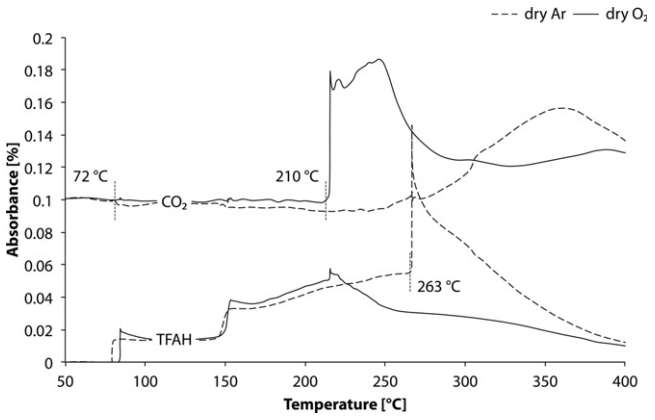

Fig. 8. Evolution of FT-IR absorbances of TFAH (1203 cm^{-1}) and CO_2 (2362 cm^{-1}) as a function of temperature during HR-TG of Cu-TFA under flowing dry Ar and O_2 atmospheres, revealing a clear difference in the decomposition reaction path (curves offset for clarity).

Analysis of the TG-DSC curves (Fig. 9) in all the atmospheres revealed the presence of two endothermic peaks (a, b) and a broad endothermic feature (c) in the temperature range below the main decomposition temperature, followed by an endothermic peak (d) or a number of overlapping exothermic peaks (d′) for the dry Ar and both O_2 atmospheres respectively. There is also a small endothermic peak (e) at a higher temperature, corresponding to the point at which the TG curve reaches its horizontal plateau, in all three atmospheres. Accurate temperature determination for each DSC peak was difficult, because the DSC base line was not straight.

To aid data interpretation, a thermal study of the starting material by means of hot stage microscopy in static air was conducted. Heating with a rate close to 50 °C/min revealed the salt, initially a blue powder, to dissolve in its own water of crystallisation and immediately released a vapour, known from FT-IR to be TFAH, at a temperature around 75 °C, i.e. corresponding to the first endothermic peak (a) in DSC. The resulting blue–green solid turned completely into a dark solid with the next TFAH liberation in the temperature range of the second endothermic peak (b). Further heating established a viscous melt, constantly releasing additional TFAH, which was associated with the third broad endothermic peak (c). It is probable that the same reaction corresponding to peak (b) is incomplete and continuing in this region with slower kinetics as a result of the reduction in surface area of the sample due to the viscous melt formation. In this temperature region the vaporisation of a copper species is most likely also taking place. The next peak (d or d′) corresponds to the decomposition of $Cu(CF_3COO)_2{\cdot}CuO$. In the hot stage microscopy experiment, violently bursting bubbles were observed until a solid black product, expected from XRD to be CuO, was formed. This

violent process is consistent with the overlapping exothermic peaks (d′) and irregular features in TG observed for decomposition in flowing O_2 atmospheres. In contrast, in flowing Ar an endothermic peak (d) is observed.

The final small endothermic peak (e) at 310 °C and 320 °C is most likely the effect of the decomposition and removal of the last remaining fluorinated organic residue around the forming CuO grains. The DSC results are in agreement with TG and HR-TG, where two sharp features associated with TFAH liberation, and a slower one from the partially hydrated salt, were defined in all three atmospheres; followed by the single and multistage decomposition of $Cu(CF_3COO)_2{\cdot}CuO$ in dry Ar and both O_2 atmospheres respectively, at comparable temperatures; and with a small but measurable mass loss near the temperature of the final endothermic peak.

4. Discussion

The FT-IR results, combined with DSC and HR-TG, provide clear evidence of the reaction routes in Ar and O_2 atmospheres. In all atmospheres, the low temperature behaviour (up to around 210 °C) is identical. In this region, FT-IR indicated that only TFAH was liberated. The first mass loss in HR-TG, near the boiling point of TFAH, was revealed by hot stage microscopy to be associated with the release of water (Reaction (1)) and the immediate hydrolysis of the salt (Reaction (2)): this suggests the limited chemical stability of the starting material. The 2:1 molar ratio between the anhydrous salt and water in Reaction (2) corresponds closely with the supplier's specified amount of water of crystallisation, so in this case no separate dehydration signal could be identified. Dihydrate [28] and trihydrate [11] Cu-TFA salts have previously been reported. However, the discrepancy in the number of water molecules bound to the salt may arise both from differences in the synthesis and the exceptional hygroscopy of the salt [10].

The solid product of Reaction (2), $Cu_2(CF_3COO)_3(OH)$, decomposes to $Cu(CF_3COO)_2{\cdot}CuO$ with a further increase of temperature (143–149 °C from HR-TG), again releasing TFAH (Reaction (3)). $Cu_2(CF_3COO)_3(OH)$ and a hydrated form of $Cu(CF_3COO)_2{\cdot}CuO$ were previously synthesised and characterised by Swarts [28].

Thermal studies revealed the decomposition of $Cu(CF_3COO)_2{\cdot}CuO$ to start at a temperature around 263 °C in a flowing dry Ar atmosphere (Table 3). From the HR-TG and DSC curves it can be seen that the endothermic single decomposition step is very rapid and that the formed species at about 310 °C is stable up to the maximum reached temperature of 600 °C. XRD powder analysis confirmed the final product of this decomposition to be CuO. The remaining mass after HR-TG is lower than the theoretical value for CuO, probably due to the vaporisation of a copper species.

The sublimation of Cu-TFA has previously been reported [29]. Carboxylate groups within a salt structure have the ability to coordinate a great number of atoms. Trifluoroacetates retain this ability but at the same time they manifest a higher ionicity of their M–O polar covalent bonds [30]. The enhanced bond allows the complexes of Cu and TFA groups to sublime at elevated temperatures and normal pressure instead of decomposing in the first instance. A strong cation–anion interaction in the case of copper(II) perchlorate ($Cu(ClO_4)_2$) due to the presence of chlorine, another electronegative element, is also known to be responsible for that salt's sublimation [9]. In the previous report, the sublimation of Cu-TFA in dry O_2 and vacuum was confirmed by Diffuse Reflectance Infrared Fourier Transform Spectroscopy (DRIFTS); this was suppressed by the introduction of water vapour, and it was suggested that this was due to hydrolysis of the salt [29]. This is broadly consistent with the behaviour in the present work, in that vaporisation was not observed in a wet O_2 atmosphere, and it has been confirmed here that hydrolysis does indeed occur. However, hydrolysis also occurred in the nominally dry O_2 and Ar atmospheres, and evidence of vaporisation of a copper species was still found in the latter case. It is possible that, in the present work, some $Cu(CF_3COO)_2{\cdot}CuO$ divides before its decomposition begins, forming anhydrous Cu-TFA which then vaporises.

Given that the solid product is known to be CuO, it would be natural to expect the decomposition of $Cu(CF_3COO)_2{\cdot}CuO$ in Ar to liberate TFAA (Reaction (4)). However, TFAA was not detected and both TFAH and HF are observed in the FT-IR spectra during the decomposition of $Cu(CF_3COO)_2{\cdot}CuO$. Even in the supposedly dry atmosphere and in the absence of any other proton source, it must be proposed that water was still present in the system, and that TFAH is formed from its heterogeneous reactions with $Cu(CF_3COO)_2{\cdot}CuO$ (Reaction (5)).

In flowing dry and wet O_2 atmospheres, thermal studies revealed the decomposition of $Cu(CF_3COO)_2{\cdot}CuO$ to start at a temperature about 50 °C lower than that in flowing dry Ar (Table 3). From the HR-TG and DSC curves it can be seen that the decomposition is highly exothermic, and hot stage microscopy confirms that violent bubbling of the viscous intermediate occurs. As in the dry Ar atmosphere, the final species formed at about 320 °C remains stable to the maximum temperature tested, and was confirmed by XRD to be CuO. The remaining mass from thermogravimetry is only in good agreement with the theoretical value for CuO in the case of HR-TG in flowing O_2 atmospheres: this may suggest that the vaporisation of copper species can been suppressed in O_2 atmospheres with a suitably slow heating rate.

From FT-IR spectroscopy, the decomposition of $Cu(CF_3COO)_2{\cdot}CuO$ in both flowing O_2 atmospheres is associated with the production of HFPO, COF_2 and CO_2 (Figs. 7 and 8). A summary reaction producing CuO and these volatile species is proposed as Reaction (6). All known methods for the synthesis of HFPO are based on the reaction of hexafluoropropene (HFP, $CF_3CF{=}CF_2$) with an oxygen donor, the reaction with molecular oxygen (O_2) requiring either thermal activation, the use of energetic radiation or the addition of radical forming agents [31–33]. It is therefore probable that the decomposition in this system proceeds via the liberation of HFP and its immediate exothermic oxidation to HFPO (Reaction (7)). The main by-products reported in the literature for this oxidation process are COF_2 (Reaction (8)), CF_3COF and hexafluoroacetone (HFA, $CF_3{-}CO{-}CF_3$), which may be present in various proportions according to the synthesis conditions; only the first was observed here. HFPO can isomerise to pentafluoropropionyl fluoride (PPF, CF_3CF_2COF) or hexafluoroacetone (HFA) [31–33]; react with water to form a monohydrate of trifluoropyruvic acid ($CF_3{-}CO{-}COOH{\cdot}H_2O$) [34]; or thermally decompose to: CF_2 and CF_3COF (Reaction (9)) [24,25,33,35]; but FT-IR suggests that none of these processes took place in the present work. A detailed investigation of the reaction mechanism of the $Cu(CF_3COO)_2{\cdot}CuO$ oxidative decomposition is beyond the scope of this work, but Reaction (6) is consistent with the FT-IR data.

In all atmospheres, HF is detected by FT-IR. One source of this, common to all the tested atmospheres, is the decomposition of TFAH (Reaction (10)), which also liberates CO_2 and produces a very reactive difluoromethylene diradical ($:CF_2$) [36]. This process is more significant for the Ar atmosphere than the O_2 atmospheres because TFAH is liberated by the main decomposition reaction; and FT-IR confirms that CO_2 and HF release lags behind this decomposition process (Fig. 8). In the wet O_2 atmosphere, an additional source of HF is the reaction of COF_2 with water, which forms a substantial amount of CO_2 and HF (Reaction (11)) [14,37,38].

The existence of: CF_2 has previously been suggested in several related systems, including a TFAH scavenging reaction with Br_2 [20] and TFAH pyrolysis in the presence of flowing Br_2 [21]; in each

case, CF_2Br_2 was identified in the IR spectrum. Furthermore, pyrolysis of a TFAH and HCl mixture has been shown (by IR) to produce $CHClF_2$ [39], and trimethyltrifluoromethyltin ($(CH_3)_3SnCF_3$) [40] with Ba-TFA [27] have been reported to produce:CF_2 on decomposition.

Some of the:CF_2 and HF combines to form CHF_3 (Reaction (12)) [14], which is not unexpected given the previously reported reactivity of:CF_2 with HCl [39]. It has also been reported that, in the absence of other reagents,:CF_2 disappears irreversibly by forming a dimer (Reaction (13)) and higher polymers [36,39,41], but neither were detected by FT-IR. The remaining:CF_2 and HF both react with the quartz elements of the furnace tube or the glass spectroscopic cell to form SiF_4 (Reaction (14) and Reaction (15) respectively) [14,36,38]. The SiF_4 absorbance is much larger for the wet O_2 atmosphere than in the dry atmospheres, suggesting that the hydrolysis of COF_2 is the primary source of HF.

$$Cu(CF_3COO)_2{\cdot}0.5H_2O = Cu(CF_3COO)_2 + 0.5H_2O \quad (1)$$

$$2Cu(CF_3COO)_2 + H_2O = Cu_2(CF_3COO)_3(OH) + CF_3COOH \quad (2)$$

$$Cu_2(CF_3COO)_3(OH) = Cu(CF_3COO)_2{\cdot}CuO + CF_3COOH \quad (3)$$

$$Cu(CF_3COO)_2{\cdot}CuO = 2CuO + (CF_3CO)_2O \quad (4)$$

$$Cu(CF_3COO)_2{\cdot}CuO + H_2O = 2CuO + 2CF_3COOH \quad (5)$$

$$4Cu(CF_3COO)_2{\cdot}CuO + (4 - x)O_2 = 8CuO + xCF_3(CFCF_2)O + (12 - 3x)COF_2 + 4CO_2 \quad (6)$$

$$CF_3CF = CF_2 + 0.5O_2 = CF_3(CFCF_2)O \quad (7)$$

$$CF_3CF = CF_2 + 1.5O_2 = 3COF_2 \quad (8)$$

$$CF_3(CFCF_2)O = : CF_2 + CF_3COF \quad (9)$$

$$CF_3COOH = : CF_2 + CO_2 + HF \quad (10)$$

$$COF_2 + H_2O = 2HF + CO_2 \quad (11)$$

$$: CF_2 + HF = CHF_3 \quad (12)$$

$$2 : CF_2 = C_2F_4 \quad (13)$$

$$2 : CF_2 + SiO_2 = SiF_4 + 2CO \quad (14)$$

$$4HF + SiO_2 = SiF_4 + 2H_2O \quad (15)$$

$$2CuO = Cu_2O + 0.5O_2 \quad (16)$$

In the O_2 atmospheres, the final solid products at both 600 °C (after HR-TG) and 1000 °C (after TG) were identified by XRD as pure CuO. In the dry Ar atmosphere, the reduction of CuO to Cu_2O started at a temperature around 700 °C (Reaction (16)), as confirmed by TG and XRD. It is likely this reduction proceeded to completion, and any CuO remaining in the product was the result of partial reoxidation when the sample was cooled in air.

In the complete absence of water, it is expected that Reaction (5) and Reaction (10) to Reaction (15) would not occur in a flowing dry Ar atmosphere. This mechanism would then be in agreement with the previously reported IR analysis of the gas mixture evolved during Cu-TFA decomposition in air under reduced pressure, containing mainly TFAA and its products of thermal decomposition [8].

The onset temperatures found in this work for the main decomposition step of Cu-TFA – 263 °C in dry Ar, 216 °C in dry O_2 and 209 °C in wet O_2 – are significantly lower than many previous reports. Baillie et al. [8] reported decomposition at 270 °C in air; Gupta et al. [1] reported the decomposition to start close to 300 °C in a flowing dry Ar atmosphere, forming a mixture of CuF_2, CuO and Cu_2O, and at a temperature 30–70 °C lower when carried out in a flowing dry O_2 atmosphere, forming CuF_2 and CuO as the final products. The onset temperatures in O_2 are even lower than the 220 °C onset in air reported by Finlayson et al. [42] during pyrolysis of a thin YBCO sol–gel film (for which lower reaction temperatures are typically expected). Baillie et al. [8] claimed in addition the formation of a small amount of involatile fluorocarbon impurities during the decomposition of Cu-TFA; no evidence of impurities was found in the CuO formed in the present work by XRD powder analysis or by transmission FT-IR.

As the TFA salts of many elements, including Y and Ba, decompose to metal fluorides below 600 °C [27,43], it might be expected that this would also be the case for Cu-TFA, and indeed CuF_2 has sometimes been reported amongst the decomposition products [1,8]. However, no CuF_2 was observed in the present work or a previous study using Raman spectroscopy [42], and the formation of oxides from the decomposition of Ni-TFA has also been reported [44].

In sol–gel processing routes, too high a heating rate around the decomposition temperature results in rapid pyrolysis, often causing cracking and porosity of the developing film. Accurate knowledge of the decomposition temperature is therefore essential to design an appropriate heat treatment. Designing a heat treatment assuming the almost 60 °C higher temperatures previously reported would be likely to result in poor coating morphology, especially in combination with the violent bubbling observed here by hot stage microscopy (which is likely to occur in typical wet O_2 processing environments).

5. Conclusions

The decomposition of $Cu(CF_3COO)_2{\cdot}0.5H_2O$ has been investigated in flowing dry Ar and both wet and dry flowing O_2. It has been determined by HR-TG coupled with FT-IR and hot stage microscopy that the salt is first hydrolysed, releasing TFAH and forming $Cu_2(CF_3COO)_3(OH)$, which subsequently decomposes to $Cu(CF_3COO)_2{\cdot}CuO$ with the further release of TFAH. Decomposition to CuO in dry Ar takes place in one endothermic stage, producing TFAH due to the presence of traces of water; no TFAA was detected. In both O_2 atmospheres, the decomposition to CuO proceeds via a number of exothermic steps: HFP and CO_2 are liberated, but the former is immediately oxidised to HFPO, and COF_2 is detected as a by-product. The presence of water causes the formation of other fluorinated species – CHF_3 and HF – and the presence of:CF_2 is also inferred. The decomposition temperatures of 263, 216 and 209 °C in flowing dry Ar, dry O_2 and wet O_2 respectively were significantly lower than previously reported. The reduction of CuO to Cu_2O takes place only in the presence of an Ar atmosphere, at around 770 °C. The mechanism of Cu-TFA decomposition proposed for the first time in this work is different from the one earlier discussed by the authors for Ba-TFA [27] and Y-TFA salts [43].

References

[1] A. Gupta, R. Jagannathan, E.I. Cooper, E.A. Giess, J.I. Landman, B.W. Hussey, Appl. Phys. Lett. 52 (1988) 2077–2079.
[2] P.C. McIntyre, M.J. Cima, M.F. Ng, J. Appl. Phys. 68 (1990) 4183–4187.
[3] S. Sathyamurthy, K. Salama, J. Supercond. 11 (1998) 545–553.
[4] S.M. Mukhopadhyay, J. Su, V. Chintameneni, J. Electron. Mater. 36 (2007) 1243–1251.
[5] Y. Tokunaga, T. Honjo, T. Izumi, Y. Shiohara, Y. Iijima, T. Saitoh, T. Goto, A. Yoshinaka, A. Yajima, Cryogenics 44 (2004) 817–822.
[6] P. Vermeir, I. Cardinael, M. Backer, J. Schaubroeck, E. Schacht, S. Hoste, I. Van Driessche, Supercond. Sci. Technol. 22 (2009) 075009.
[7] A. Llordes, K. Zalamova, S. Ricart, A. Palau, A. Pomar, T. Puig, A. Hardy, M.K. Van Bael, X. Obradors, Chem. Mater. 22 (2010) 1686–1694.
[8] M.J. Baillie, D.H. Brown, K.C. Moss, D.W.A. Sharp, J. Chem. Soc. A (1968) 3110–3114.

[9] M.J. Baillie, D.H. Brown, K.C. Moss, D.W.A. Sharp, J. Chem. Soc. A (1968) 104–107.
[10] R.C. Thompson, D.B. Yawney, Can. J. Chem. 43 (1965) 1240–1242.
[11] K.S. Patel, J.A. Faniran, J. Inorg. Nucl. Chem. 38 (1976) 1001–1005.
[12] C.A. Agambar, K.G. Orrell, J. Chem. Soc. A (1969) 897–904.
[13] G.R. Heal, P.J. Haines (Eds.), Principles of Thermal Analysis and Calorimetry, The Royal Society of Chemistry, Cambridge, 2002, pp. 10–54.
[14] D.M. Jollie, P.G. Harrison, J. Chem. Soc., Perkin Trans. 2 (1997) 1571–1575.
[15] G.A. Kuipers, D.F. Smith, A.H. Nielsen, J. Chem. Phys. 25 (1965) 275–279.
[16] C.J. Pouchert, The Aldrich Library of FT-IR Spectra Vapor Phase, first ed., Aldrich Chemical Company Inc., Milwaukee, 1989.
[17] R.L. Redington, Spectrochim. Acta A 31 (1975) 1699–1705.
[18] R.E. Kagarise, J. Chem. Phys. 27 (1957) 519–522.
[19] J. Pola, Z. Bastl, J. Tlaskal, Infrared Phys. 30 (1990) 355–357.
[20] R.A. Mitsch, J. Heterocyclic Chem. 1 (1964) 223–234.
[21] T. Shimanouchi, J. Phys. Chem. Ref. Data 6 (1977) 993–1103.
[22] C.V. Berney, A.D. Cormier, Spectrochim. Acta A 28 (1972) 1813–1822.
[23] N.C. Craig, Spectrochim. Acta A 44 (1988) 1225–1226.
[24] W. Mahler, P.R. Resnick, J. Fluorine Chem. 3 (1973) 451–542.
[25] C.B. Labelle, S.M. Karecki, R. Reif, K.K. Gleason, J. Vac. Sci. Technol. A 17 (1999) 3419–3428.
[26] K.W. Rillings, J.E. Roberts, Thermochim. Acta 10 (1974) 285–298.
[27] M. Mosiadz, K.L. Juda, S.C. Hopkins, J. Soloducho, B.A. Glowacki, Thermochim. Acta 513 (2011) 33–37.
[28] F. Swarts, Bull. Soc. Chim. Belg. 48 (1939) 176–192.
[29] P.C. Mcintyre, R.C. Chiu, M.J. Cima, W.E. Rhine, Mater. Res. Soc. Symp. Proc. 169 (1989) 743–746.
[30] S.I. Gutnikov, E.V. Karpova, M.A. Zakharov, A.I. Boltalin, Russ. J. Inorg. Chem. 51 (2006) 541–548.
[31] H. Millauer, W. Schwerrtfeger, G. Siegemund, Angew. Chem., Int. Ed. Engl. 24 (1985) 161–179.
[32] G. Siegemund, W. Schwertfeger, A. Feiring, G. Smart, F. Behr, H. Vogel, B. McKusick, in: Wiley-VCH (Ed.), Ullmann's Encyclopedia of Industrial Chemistry, Wiley-VCH, Verlag GmbH & Co KGaA, Weinheim, 2002.
[33] P. Tarrant, C.G. Allison, K.P. Barthold, E.C. Stump, P. Tarrant (Eds.), Fluorine Chemistry Reviews, Marcel Dekker, New York, 1971, pp. 77–113.
[34] D. Sianesi, A. Pasetti, F. Tarli, J. Org. Chem. 31 (1966) 2312–2316.
[35] H.S. Eleuterio, J. Macromol. Sci. A 6 (1972) 1027–1052.
[36] J. Pola, Collect. Czech. Chem. Commun. 46 (1981) 2854–2859.
[37] C. George, J.Y. Saison, J.L. Ponche, P. Mirabel, J. Phys. Chem. 98 (1994) 10857–10862.
[38] P.G. Blake, H. Pritchard, J. Chem. Soc. B (1967) 282–286.
[39] W. Mahler, Inorg. Chem. 2 (1963) 230.
[40] H.C. Clark, C.J. Willis, J. Am. Chem. Soc. 82 (1960) 1888–1891.
[41] P.J. Corbett, E. Whittle, J. Chem. Soc. (1963) 3247–3251.
[42] A.P. Finlayson, T. Mouganie, M.C. Cordero-Cabrera, B.A. Glowacki, Mater. Chem. Phys. 105 (2007) 99–104.
[43] M. Mosiadz, K.L. Juda, S.C. Hopkins, J. Soloducho, B.A. Glowacki, J. Therm. Anal. Calorim. (2011), doi:10.1007/s10973-011-1772-6.
[44] H.K. de Souza, E.A. Sousa, M.D. Paiva, F.M. Borges, D.M. Melo, H. Scatena Jr., J. Therm. Anal. Calorim. 93 (2008) 959–962.